Braz J Phys (2015) 45:72–78
DOI 10.1007/s13538-014-0298-3

STATISTICAL

Effect of Surface Oxide Transformation on CO Oxidation

I. Sinha · A. K. Mukherjee

Received: 21 January 2014 / Published online: 6 January 2015

Abstract Under sub-atmospheric conditions, many metal catalyst surfaces for CO oxidation transform to the oxide phase with higher catalytic activity than chemisorbed oxygen. The surface phase transformation from metal to its oxide could be by collective oxidation of the adsorbed oxygen sites as soon as their coverage reaches a global critical threshold, or such oxidation may be restricted to small patches of the surface, which is driven by the local coverage. In this communication, we investigate the effect of the latter on the phase diagram and the CO_2 production rate behavior using a kinetic Monte Carlo surface reaction lattice gas model for CO oxidation.

Keywords Catalytic surface reactions · Kinetic Monte Carlo simulations · CO oxidation · Surface oxide

1 Introduction

A variety of models have been proposed for different surface reaction phenomena such as chaotic behavior, bistability, critical phenomena, out-of-equilibrium phase transitions, etc. Among these, the non-equilibrium or irreversible phase transitions (IPTs) in the preferred model surface catalysis case of CO oxidation reaction have primarily been investigated by different variants of Ziff-Gulari-Barshad (ZGB) model [1]. Because the focus is on understanding of IPT, therefore, a simplified approach to modeling of catalytic oxidation of CO is adopted in the ZGB model. In this model, the single crystal catalytic surface is assumed to be a two-dimensional square lattice with periodic boundary conditions. The model then proceeds according to the Langmuir–Hinshelwood (LH) mechanism [2]. Thus, reactants CO and O_2 are selected for adsorption on to the catalyst surface with normalized probabilities P_{CO} and P_{O_2} which are proportional to respective reactant partial pressures. If CO molecule is selected, then it may adsorb onto a vacant site. Alternatively, the oxygen molecule first dissociates into atoms and then may get adsorbed onto two neighboring vacant sites. If adjacent sites are occupied by O and CO molecules, then they react instantaneously to form CO_2, which desorbs leaving behind two empty sites. All mentioned processes are irreversible once they occur. The catalyst surface CO coverage as well as CO_2 production rate varies with normalized partial pressures of CO. Two IPTs are exhibited in this phase diagram between CO coverage and P_{CO}. For P_{CO} values less than a lower threshold (P_1), the surface is oxygen poisoned. Further, for P_{CO} values greater than an upper threshold (P_2), the surface is CO poisoned. Therefore, reaction between CO and O_2 occurs only in a narrow range P_{CO} values between P_1 and P_2. While the oxygen poisoning transition is continuous, the phase transition to the CO-poisoned state is discontinuous. However, real systems do not show the second-order transition to an oxygen-poisoned state [3–5], while discontinuous transitions between states of low and high CO coverage have been observed experimentally [6]. Many facets of surface-catalyzed reactions have been investigated on the ZGB phase diagram and the discontinuous phase transition. These include propagation and fluctuation behavior of interfaces between active and poisoned states [1, 7, 8], epidemic properties of an active droplet embedded in the poisoned state [9, 10], nucleation of droplets within the metastable active state [7, 11] as well as effect of oscillatory reaction kinetics [12] on the ZGB discontinuous phase transition. The present paper investigates a kinetic Monte Carlo model in the ZGB framework for

I. Sinha (✉) · A. K. Mukherjee
Department of Chemistry, Indian Institute of Technology (Banaras Hindu University), Varanasi 221005, India
e-mail: isinha.apc@itbhu.ac.in

investigating the effect of formation of a more reactive surface oxide phase on the consequent phase diagram.

A lacuna with studies on surface-catalyzed reactions is due to low/ultrahigh vacuum (UHV) pressures (10^{-9}bar) used in CO oxidation model experiments. These do not describe the pressures applied in practical catalysis (>1 bar). Under UHV conditions, LH reaction occurs between CO and O_2 adsorbed on the adjacent vacant sites on the catalyst surface. The CO_2 production rate and the adsorbate coverages exhibit oscillatory kinetics due to surface reconstruction. For instance, catalytic oxidation of CO on Pt-group metal surfaces displays oscillatory kinetics UHV conditions. The non-reconstructed surface phase Pt(1×1 structure) shows CO oxidation activity while the reconstructed hex Pt(1×2) phase does not [3, 13–15].

However, under sub-atmospheric pressure conditions CO, oxidation on Pd(100) happens by spontaneous cycles of collective oxidation and reduction of the metal surface [16–19]. The relatively less stable surface oxide phase has comparatively better catalytic activity. While under reducing conditions, the catalyst surface exhibits lower activity characteristic of a CO-covered metallic surface. Gustafson et al. also found that at high P_{O_2} conditions, CO oxidation over Rh(111) and (100) results in high CO_2 production rate consequent to the catalyst surface oxide phase formation [20]. Investigations by other authors on CO oxidation using heterogeneous catalysts have also demonstrated that surface oxide formation occurs with CO_2 formation rate. Similar observations have also been reported for the CO oxidation over Pt(110) at higher pressure (0.5 Torr of O_2). Nanometer-sized islands of multilayered α-PtO_2-like surface oxide form along with chemisorbed oxygen [21].

Based on experimental evidence, these investigators primarily proposed that chemisorbed oxygen may react only by LH mechanism, but besides this, the surface oxide can also directly react with the gas phase CO molecule by the Mars–van Krevelen (MvK) mechanism [22]. Rate oscillations are therefore a consequence of alternating between slower LH oxidation kinetics of CO and faster oxide kinetics. In a recent kinetic Monte Carlo study [23], we simulated this sub-atmospheric pressure condition mechanism of surface-catalyzed CO oxidation. This model utilized a modified Ziff-Gulari-Barshad lattice gas model [1] framework. While the chemisorbed oxygen follows the LH mechanism, the surface oxide can react with an adjacent CO-occupied site or directly react with the gas phase CO molecule as per the MvK mechanism. The collective oxidation/reduction phenomena as suggested for CO oxidation on Pd(100) was modeled by introducing a critical threshold (CT) of oxygen coverage above which all adsorbed oxygen sites were assumed to transform globally to the more reactive surface oxide phase. Rate oscillations were observed because of the coupling between the slower LH reactions with the faster oxide kinetics. The long time average of the oscillating reactant coverages and the CO_2 production rate were plotted against the normalized CO partial pressure (P_{CO}). Depending on the CT value at which the phase diagram is simulated, two or three phase transitions with respect to the reactant coverage order parameters may be observed. Moreover, the discontinuous transition from the reactive to CO-poisoned state occurs at a P_{CO} value very near to the classical ZGB model poisoning transition point [1, 12].

In the aforementioned model, we assumed that all adsorbed oxygen transform to surface oxide globally as the overall surface oxygen coverage of the catalyst single crystal reached a critical value. However, the surface oxide transformation could occur collectively in two ways. This may be either by collective oxidation of oxygen-occupied sites throughout the system as soon as the CT is reached globally (that is throughout the single crystal) or whenever the CT is reached in small patches of oxygen-occupied sites. In the present study, we implement the second case, that is, the surface oxide transformation is now restricted to small patches of the surface and is driven by the local coverage. We investigate the effect of the size of such surface oxide patches on the kinetics of CO oxidation and compare results to those for global oxidation and reduction of the overall catalyst surface. As in reference [23], here, also the long time average of the oscillating reactant coverages and the CO_2 production rate are plotted against the normalized CO partial pressure (P_{CO}) giving phase diagrams which show different regimes of CO oxidation activity. The effect of the mechanism of surface oxide phase transformation on such phase diagram is thus considered.

2 Simulation Procedure

The model system is a two-dimensional square lattice of side L (=100) which is representative of a typical (100) surface. Periodic boundary conditions are employed throughout the simulation. Each simulation starts from an empty lattice. The system evolves in units of Monte Carlo steps. One Monte Carlo step (MCS) of our simulation involves L^2 trials. A trial begins by choosing either CO or O_2 for adsorption attempt on the surface. Reactants CO and O_2 are adsorbed on the surface of the catalyst with normalized probabilities P_{CO} and P_{O_2} (that is $P_{CO}+P_{O_2}=1$) proportional to the respective reactant partial pressures. If the trial consists of the CO molecule from the gas phase, then it may adsorb onto a vacant lattice site. On the other hand, the oxygen molecule first dissociates into two atoms and then may get adsorbed onto two neighboring vacant sites. As per the LH mechanism, if adjacent sites are occupied by O and CO molecules, then they react to form CO_2

leaving behind two empty sites. The complete reaction scheme including the subsequent steps followed in the model is as given below.

$$CO(g) + S \rightarrow CO_{(ads)}, \quad (1)$$

$$O_2(g) + 2S \rightarrow 2O_{(ads)}, \quad (2)$$

$$CO_{(ads)} + O_{(ads)} \rightarrow CO_2(g) + 2S, \quad (3)$$

$$O_{(ads)} \rightarrow ox\left(for\ each\ patch\ under\ the\ condition\ \theta^{local}_{O(ad)} \geq CT\right), \quad (4)$$

$$CO(g) + ox\ CO_2(g) + S, \quad (5)$$

$$CO_{(ads)} + ox\ CO_2(g) + S. \quad (6)$$

Here, the (ads) and (g) indices denote the adsorbed and gaseous species, respectively, while "S" and ox denote the vacant lattice and oxide sites, respectively. To model step (4), we divide the lattice of size $L \times L$ into small patches of size $L_P \times L_P$ [24]. Each atom of the dimer O_2 may adsorb on

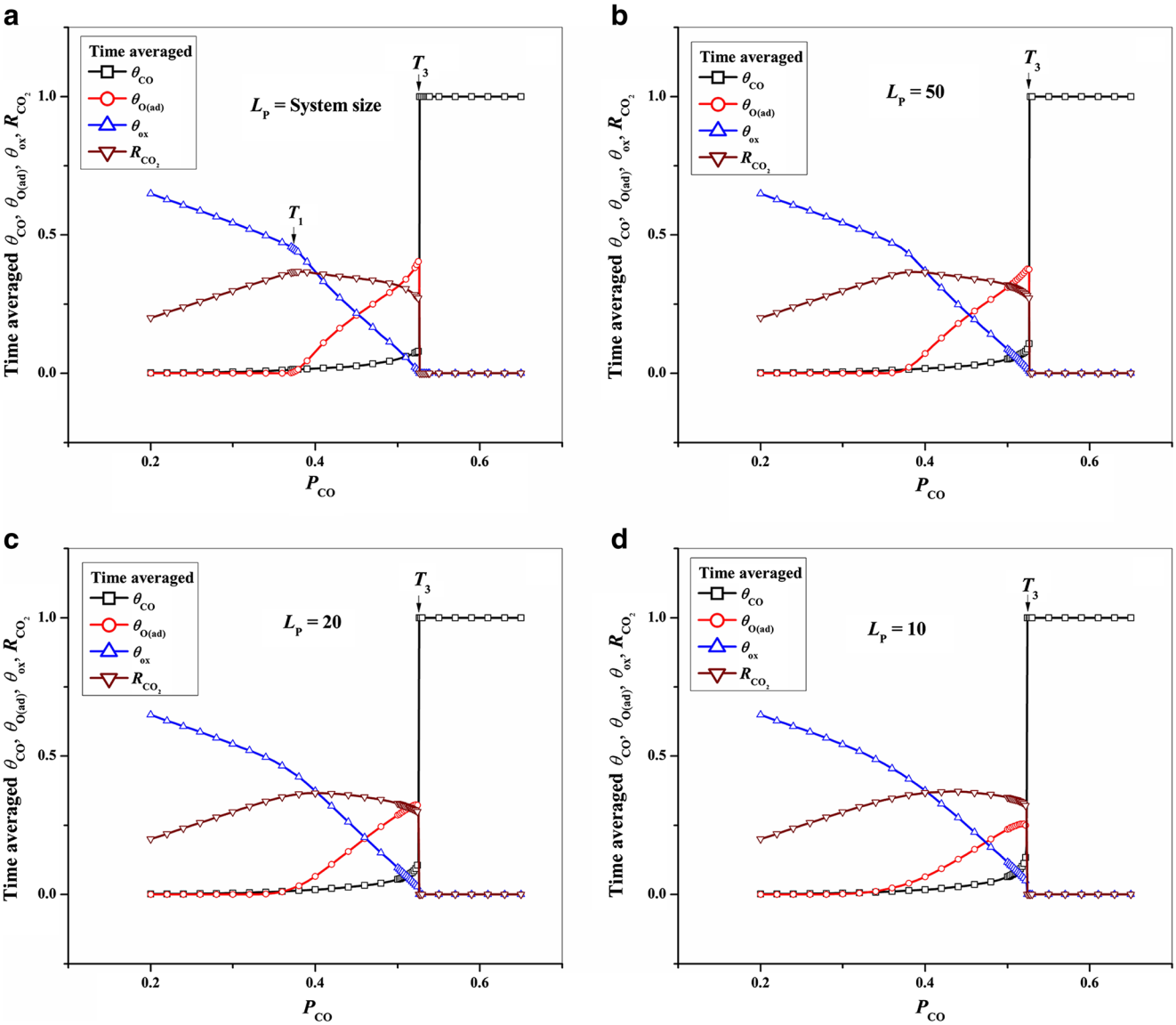

Fig. 1 Phase diagrams showing plots of $\overline{R}_{CO_2}$ $\overline{\theta}_{CO}$, $\overline{\theta}_{O(ad)}$, $\overline{\theta}_{ox}$ versus P_{CO} at CT=0.45. Surface oxide phase transformation governed by **a** global surface oxide transformation, **b** patch size L_p=50, **c** patch size L_p=20, and **d** patch size L_p=10

neighboring sites in either the same or adjacent patches. Neighboring CO- and O-occupied sites on different patches are also allowed to react. In this way, correlations may develop through the whole sample via neighboring patches. Now, the surface oxide phase transformation is governed by the CT value of adsorbed oxygen coverage $\theta_{O(ad)}$ in each local patch. Therefore, in each patch. as soon as local coverage $\theta_{O(ad)}^{local}$ exceeds CT. then all adsorbed oxygen atoms in the patch convert into surface oxide sites. Once a site is converted into oxide, it remains so until reduced back to the metallic state by either step (5) or (6). Thus, oxide sites may be reduced by the MvK mechanism which involves a gas CO molecule striking an oxide site to reduce it to the metallic state with the formation of a CO_2 molecule. The other alternative is that if the site neighboring the oxide is CO occupied, then the two react to form CO_2, leaving behind two empty metallic sites. We abbreviate the possibility of MvK step (5) and step (6) both occurring in the system as mMvK. The reduction of oxide sites by the indicated mechanisms lead to decrease in oxygen coverage of the patch. Subsequently, CT is compared with the total oxygen coverage (θ_O) of the patch. The latter is a sum of two components—adsorbed oxygen (afresh)+oxide coverage. In case θ_O falls below the required CT, then $\theta_{O(ad)}$ remains in that form and may only be reduced by the LH mechanism. The remaining oxide sites (if any) may react either by step (5) or (6).

3 Results and Discussion

In the results discussed, we denote the global CO coverage, surface oxide coverage, adsorbed oxygen coverage, and CO_2 production rate by θ_{CO}, θ_{ox}, $\theta_{O(ad)}$, and R_{CO_2} respectively. The long time averages of these quantities (denoted by $\overline{\theta}_{CO}$, $\overline{\theta}_{ox}$, $\overline{\theta}_{O(ad)}$ and $\overline{R}_{CO_2}$) at different P_{CO} values are used to construct the phase diagram of the system at a given CT. For computation of the long time average quantities, the first 3.5×10^4 time steps (or MCS) are disregarded to allow the establishment of a stationary state. The subsequent 1.5×10^4 MCS are used to compute the long time average quantities. The phase diagram of the system (at the considered CT value) with respect to the P_{CO} parameter is first presented, and the effect of the patch size (L_P) is discussed. Then, we present the variation of R_{CO_2} with respect to MCS, to understand the changes in fluctuations or any oscillatory behavior with respect to L_P in a particular regime of the phase diagram.

Figure 1 shows phase diagrams obtained at CT=0.45 with different model system patch size parameters. For the sake of comparison, first, in Fig. 1a, we reproduce the phase diagram of the case where the surface oxide phase transformation mechanism is global. That is, as soon as the adsorbed oxygen coverage exceeds or equals CT=0.45, all oxygen-occupied sites transform globally (throughout the system) to oxides. As discussed in detail in reference [23], here, one observes two transitions T_1 and T_3 in $\overline{\theta}_{CO}$, $\overline{\theta}_{ox}$, $\overline{\theta}_{O(ad)}$, and $\overline{R}_{CO_2}$ parameters with change in P_{CO}. While T_1 appears to be a continuous transition, T_3 is definitely a discontinuous transition to the CO-poisoned state. The T_1 transition occurs because of a gradual change in the dominant mechanism of CO oxidation with increase in P_{CO}. In reference [23], we have discussed that the T_3 transition (~0.5263±0.0005) occurs at value very close to the classical ZGB model P_{CO} value. On the other hand, when the surface oxide phase transformation mechanism assumes large enough patch size (L_P=50) criteria, both T_1 and T_3 transitions are still there. We note that even for the smallest patch size considered (L_P=10), the discontinuous transition (T_3) is

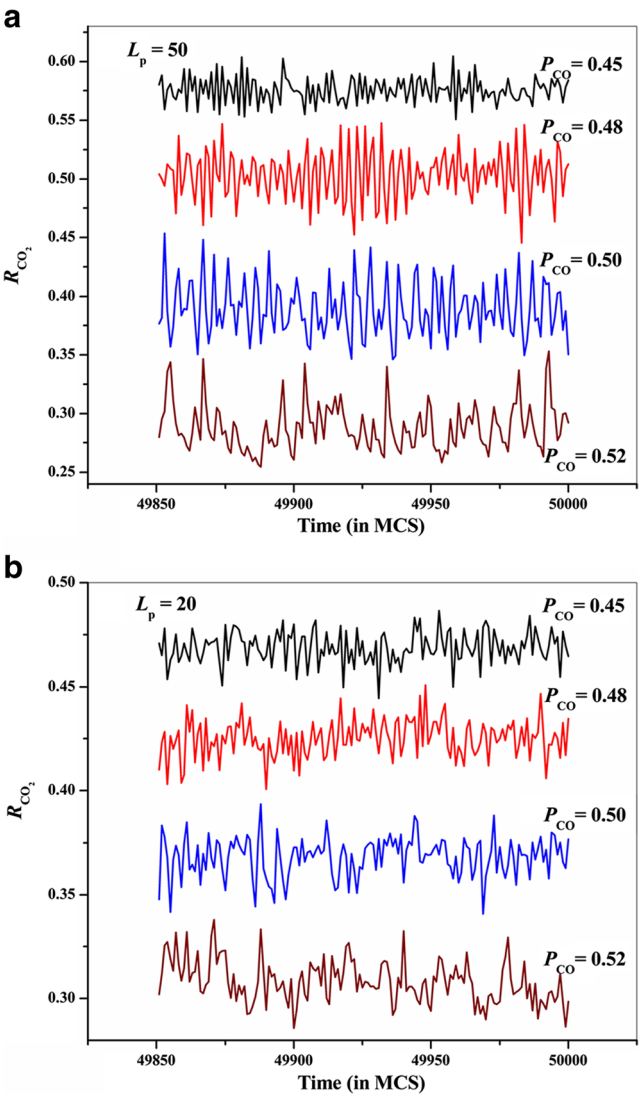

Fig. 2 Displays change in R_{CO_2} behavior with increase in P_{CO} at CT= 0.45 when the surface oxide phase transformation is governed by **a** local patch size L_p=50 and **b** L_p=20

still there. Here, it is pertinent to mention that as L_P is decreased to values <25, the discontinuous transition shifts to slightly smaller P_{CO} values. For L_P>25, the P_{CO} value at which the discontinuous transition T_3 occurs appears to be almost invariant. However, detailed statistical analysis is required before making any quantitative comments on this issue.

In Fig. 1c, the surface oxide phase transformation mechanism assumes smaller patch size (L_P=20) criteria, and T_1 is now diffuse. Further, there is no such (T_1) transition at all in Fig. 1d (L_P=10). Therefore, in contrast to the sharp T_1 transition observed in Fig. 1a, when the transformation to oxide phase is determined by local oxygen coverage, then one finds that the T_1 transition becomes diffuse as the patch size is made smaller. To understand this phenomenon better, we first following reference [23] briefly discuss Fig. 1a. In the phase diagram regime $P_{CO}<T_1$ in Fig. 1a, because of the relatively higher probability of oxygen adsorption, $\theta_{O(ad)}$ quickly exceeds CT leading to the oxidation of all oxygen occupying sites in the system. Since in this regime $CT \geq \theta_O$ always, therefore, CO oxidation only occurs by step (5) or (6) mechanisms. However, as P_{CO} is increased, at and above T_1, the mechanism of CO oxidation oscillates between the faster CO oxidation activity shown by the oxide sites and the slower LH oxidation of CO due to adjacent adsorbed oxygen sites. The T_1 transition is therefore unique and sharp only when the surface oxide transformation mechanism is determined by the global CT of oxygen coverage. On the other hand, when transformation is dictated by the local O coverage, reactions between neighboring CO- and O-occupied sites on different patches result in development of correlations through the whole sample via neighboring patches. Therefore, when the surface oxide transformation is determined by local oxygen coverage, the T_1 transition occurs at different but closely related P_{CO}

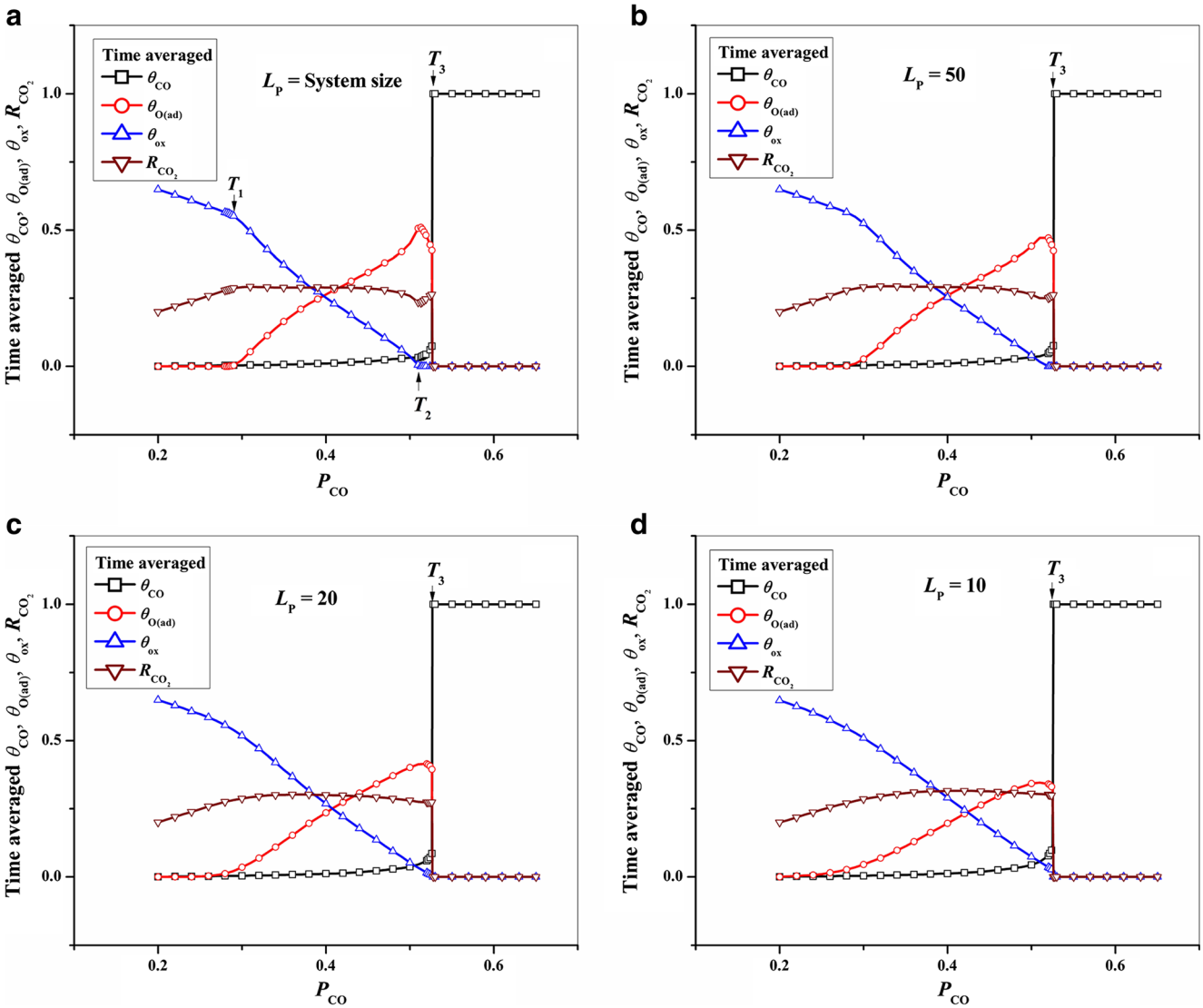

Fig. 3 Phase diagrams showing plots of $\overline{R}_{CO_2}$ $\overline{\theta}_{CO}$, $\overline{\theta}_{O(ad)}$, $\overline{\theta}_{ox}$ versus P_{CO} at CT=0.55. Surface oxide phase transformation governed by **a** global surface oxide transformation, **b** patch size L_p=50, **c** patch size L_p=20, and **d** patch size L_p=10. The transition T_2 occurs only in **a** and **b**

values in different patches. Correlations become stronger with increase in the number of patches or the consequent decrease in size of the patches. Thus, when the number of patches is small (L_P=50), the T_1 transition seems to be almost sharp, and for L_P=10, no such transition could be observed.

In Fig. 2, we present the variation of R_{CO_2} with MCS for the CT=0.45 criteria at different P_{CO} values between T_1 and T_3 transitions. Figure 2a displays these features when L_P=50 and Fig. 2b when L_P=20. Please note that depending on the amplitude of oscillations, R_{CO_2} may have values in the range from 0.28 to 0.4. To conveniently display these features, we have offset the plots at different P_{CO} values because otherwise they would overlap. The y-axis R_{CO_2} values have still been given so that one can appreciate the change in the magnitude of the variations as L_P is changed. We observe from Fig. 2a that the R_{CO_2} shows small amplitude random fluctuations at P_{CO}~0.45. The amplitude of these fluctuations increases at P_{CO}~0.48 and also seems to show some pattern with MCS where the amplitude grows from a small value to appreciable magnitudes and then again to smaller values akin to oscillatory behavior. While the amplitude of such fluctuations is maximized at P_{CO}~0.5, their periodicity is irregular. However, for P_{CO}>0.5, only small irregular fluctuations are observed, which is expected since the system approaches the irreversible discontinuous transition from reactive to CO-poisoned state. Now, we present Fig. 2b results for patch size L_P=20. When plots at the same P_{CO} values are compared, we find that the fluctuation amplitudes in Fig. 2b are still smaller (about one third) as well as irregular as compared to that in Fig. 2a. We also find that there is only small or insignificant increase in these amplitudes when P_{CO} is increased.

We now compare this behavior with the results of reference [23]. In reference [23], much clearer and better oscillatory behavior could be observed. In that model, as P_{CO} is increased, at and above T_1, the mechanism of CO oxidation oscillates between the faster CO oxidation activity shown by the oxide sites and the slower LH oxidation of CO due to adjacent adsorbed oxygen sites. The higher reactivity of the oxide phase is due to possible CO oxidation by either MvK or step (6) that leads to a jump in R_{CO_2}. Since oxide sites are very quickly reduced to metallic state, therefore θ_{ox} very quickly goes to zero [23]. On the other hand, the lower reactivity of adsorbed oxygen leads to increase in $\theta_{O(ad)}$ level with consequent decrease in R_{CO_2}. This oscillatory behavior obviously increases with P_{CO} till its value is just less than T_3. However, in the present work, the T_1 transition occurs at different but closely related P_{CO} values in different patches. This means that at a given P_{CO}, oscillations occur in different phases in different patches. This means that the more the number of patches, the more the chances of destructive interference resulting in irregular small fluctuations. Thus, the amplitude of oscillations become smaller or insignificant as the number of patches is increased.

The phase diagrams for CT=0.55 are shown in Fig. 3. As before, for the sake of comparison, Fig. 3a gives the phase diagram for global surface oxide transformation mechanism. Here, for a higher CT value, as discussed in reference [23], when P_{CO} is increased to a high enough value, there is no more surface oxide formation. This results in another continuous transition T_2. Beyond T_2, there is no more oscillatory behavior since only the LH mechanism of CO oxidation is operative. Now, in Fig. 3b for L_P=50, we observe that both T_1 and T_2 become diffuse. As we decrease L_P or increase the number of patches, this trend continues, that is, the transitions T_1 and T_2 disappear. Again, as for CT=0.45 condition for patch size L_P=50, the system exhibits almost regular fluctuations patterns in R_{CO_2} which is similar to oscillatory behavior observed in case of global surface oxide transformation [23] mechanism (Fig. 4a). However, on increasing the CO partial pressure further, the amplitude of such fluctuations become

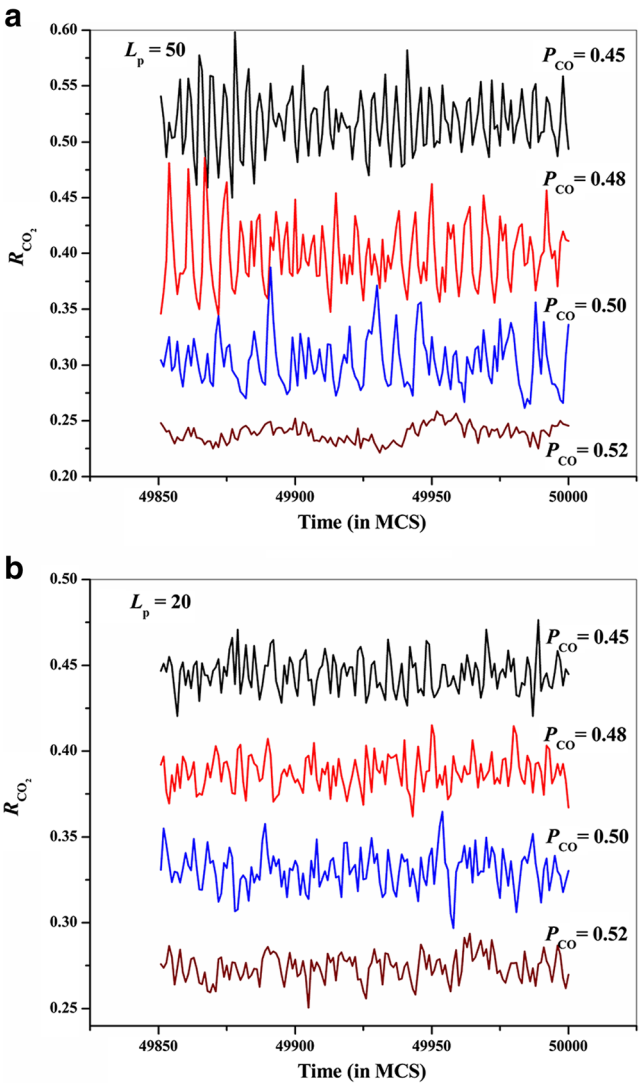

Fig. 4 Displays change in R_{CO_2} behavior with increase in P_{CO} at CT= 0.55 when the surface oxide phase transformation is governed by **a** local patch size L_p=50 and **b** L_p=20

smaller and also become irregular. Even for L_P=50, such fluctuations are exhibited only up to T_2 since beyond T_2, only the LH mechanism is operative. In case of L_P=20 (Fig. 4b), only smaller irregular amplitude fluctuation behaviors are observed because of destructive interference between P_{CO} oscillations in different phases in different patches.

4 Conclusions

Under sub-atmospheric conditions, the surface oxide transformation of metal catalyst surface for CO oxidation could occur either by collective oxidation of oxygen-occupied sites throughout the system as soon as a CT surface oxygen coverage is reached globally (that is throughout the single crystal) or whenever the CT of oxygen-occupied sites is reached in small patches of the surface. In the present study, a recent kinetic Monte Carlo surface reaction lattice gas model for CO oxidation under sub-atmospheric conditions has been modified for simulating the latter situation. As soon as the oxygen coverage in a patch exceeds this *CT* value, all adsorbed oxygen atoms in the patch convert into surface oxide sites. These surface oxide sites have higher catalytic activity than adsorbed oxygen because they can either react directly with gas phase CO molecules (MvK mechanism) or can also undergo LH type reactions with adjacent CO-occupied sites.

The results have been presented in terms of phase diagrams which are long time averages of various coverage parameters plotted against the normalized CO pressure. For large patch sizes L_P=50, we still observe transitions in the phase diagram similar to the case when collective or global surface oxide transformation mechanism [23] is considered. Thus, the phase diagrams show two or three transitions depending on the *CT* value. The first continuous T_1 transition is due to a gradual change in the dominant mechanism of CO oxidation with increase in P_{CO}. If the CT value is high, then another transition (T_2) may also be observed. Finally, when P_{CO} is increased to high enough value, there is a discontinuous transition (T_3) to a CO-poisoned state. However, on further decreasing the patch size, continuous transitions (T_1 & T_2) become diffuse and ultimately disappear. The reason being that in contrast to the global transformation mechanism, the continuous transition occurs at different but closely related P_{CO} values in different patches. Decreasing the size of the patches affects the position of the discontinuous transition as well. The pronounced oscillatory behavior observed for global surface oxide transition mechanism is also affected. The amplitude of CO_2 production rate fluctuations becomes smaller or insignificant as the number of patches is increased since oscillations in different patches are out of phase.

References

1. R.M. Ziff, E. Gulari, Y. Barshad, Phys. Rev. Lett. **56**, 2553 (1986)
2. E. Loscar, E.V. Albano, Rep. Prog. Phys. **66**, 1343–1382 (2003)
3. T. Engel, G. Ertl, Adv. Catal. **28**, 1 (1979)
4. P. Meakin, J. Chem. Phys. **93**, 2903 (1990)
5. S.S. Tambe, V.K. Jayaraman, B.D. Kulkarni, Chem. Phys. Lett. **225**, 303 (1994)
6. M. Ehsasi, M. Matloch, O. Frank, J.H. Block, K. Christmann, F.S. Rys, W. Hirschwald, J. Chem. Phys. **91**, 4949 (1989)
7. J. Marro, R. Dickman, *Nonequilibrium phase transitions in lattice models* (Cambridge University Press, Cambridge, 1999)
8. J.W. Evans, T.R. Ray, Phys. Rev. E. **50**, 4302 (1994)
9. R.H. Goodman, D.S. Graff, L.M. Sander, P. Leroux-Hugon, E. Clément, Phys. Rev. E. **52**, 5904 (1995)
10. J.W. Evans, M.S. Miesch, Phys. Rev. Lett. **66**, 833 (1991)
11. E. Machado, G.M. Buendía, P.A. Rikvold, Phys. Rev. E. **71**, 031603 (2005)
12. I. Sinha, A.K. Mukherjee, J. Stat. Phys. **146**, 669 (2012)
13. R. Imbihl, G. Ertl, Chem. Rev. **95**, 697 (1995)
14. M. Eiswirth, P. Möller, K. Wetzl, R. Imbihl, G. Ertl, J. Chem. Phys. **90**, 510 (1989)
15. R. Imbihl, M.P. Cox, G. Ertl, J. Chem. Phys. **84**, 3519 (1986)
16. M. Baerns, R. Imbihl, V.A. Kondratenko, R. Kraehnert, W.K. Offermans, R.A. van Santen, A. Scheibe, J. Catal. **232**, 226 (2005)
17. B.L.M. Hendriksen, S.C. Bobaru, J.W.M. Frenken, Top. Catal. **36**, 43 (2005)
18. B.L.M. Hendriksen, J.W.M. Frenken, Phys. Rev. Lett. **89**, 046101 (2002)
19. B.L.M. Hendriksen, S.C. Bobaru, J.W.M. Frenken, Surf. Sci. **552**, 229 (2004)
20. J. Gustafson, R. Westerstro¨m, O. Balmes, A. Resta, R. van Rijn, X. Torrelles, C.T. Herbschleb, J.W.M. Frenken, J. Phys. Chem. C **114**, 4580 (2010)
21. D.R. Butcher, M.E. Grass, Z. Zeng, F. Aksoy, H. Bluhm, W. Li, B.S. Mun, G.A. Somorjai, Z. Liu, J. Am. Chem. Soc. **133**, 20319 (2011)
22. P. Mars, D.W. van Krevelen, Spec. Suppl. Chem. Eng. Sci. **3**, 41 (1954)
23. I. Sinha, A.K. Mukherjee, Chem. Phys. Lett. **553**, 30 (2012)
24. E.V. Albano, J. Chem. Phys. **109**, 7498 (1998)